Acyl Chain Unsaturation and Vesicle Curvature Alter Outer Leaflet Packing and Promote Poly(ethylene glycol)-Mediated Membrane Fusion†

Will A. Talbot, Lian Xing Zheng, and Barry R. Lentz*

Department of Biochemistry and Biophysics, University of North Carolina, Chapel Hill, North Carolina 27599-7260

Received September 27, 1996; Revised Manuscript Received March 18, 1997⊗

ABSTRACT: The poly(ethylene glycol) (PEG)-induced fusion of sonicated, unilamellar vesicles (SUV) and large, unilamellar vesicles (LUV) composed of a variety of phosphatidylcholine species was compared using two assays for the mixing and leakage of internal vesicle contents. In the first [Lentz *et al.* (1992) *Biochemistry*, *31*, 2643], disodium 8-aminonaphthalene-1,3,6-trisulfonate (ANTS) fluorescence is quenched by co-encapsulated *N*,*N*′-*p*-xylylenebis(pyridinium bromide) (DPX). For this assay, interference by the fluorescence of impurities in PEG demands that the PEG content of the sample be reduced by dilution before measurements are taken. The second assay [Viguera *et al.* (1993) *Biochemistry*, *32*, 3708] monitors the fluorescence of Tb^{3+} complexed with dipicolinic acid (DPA) directly in concentrated PEG solutions. The two assays gave identical fusion profiles for egg PC SUVs treated with increasing concentrations of PEG, demonstrating that fusion occurs in the dehydrated state in the presence of PEG and does not require dilution. Comparison of results obtained with lipid species of varying degrees of unsaturation incorporated into either SUV or LUV suggested that acyl chain unsaturation and high membrane curvature combine to favor fusion of pure phosphatidylcholine membranes. There was a clear correlation between the fluorescence lifetime or the order parameter of the membrane probe 1-(4-trimethylammonium)-6-phenyl-1,3,5-hexatriene (TMA-DPH) in different membranes and the concentration of PEG needed to induce fusion of these membranes. However, the ratios of TMA-DPH lifetimes measured in D_2O versus H_2O buffers were the same for different lipid species, indicating that probe penetration was not very different for different lipid species. The results suggest that the combined effect of high membrane curvature and extensive chain unsaturation is an enhanced rate of lipid motion in the upper region of the bilayer, reflective of decreased packing density in the outer leaflet of unsaturated SUV bilayers, probably allowing for enhanced water penetration leading to an enhanced probability of fusion.

Poly(ethylene glycol) (PEG[1]) interacts with water and thereby lowers the activity of water in bulk solution (Bailey & Koleske, 1967). Its swollen, hydrated structure excludes it from macromolecular surfaces (Evens & Needham, 1988; Arnold *et al.*, 1990). This causes a gradient in the chemical potential of water between such a surface and bulk water, leading to a thermodynamic potential that forces the aggregation and close apposition of membrane vesicles exposed to PEG (Evens & Needham, 1988; Arnold *et al.*, 1990). Since close apposition of opposed membrane bilayers is accepted to be the first essential step in membrane fusion, PEG aggregation of model membranes has become a useful means of exploring the membrane structural perturbations that accompany biomembrane fusion (Lentz, 1994). We have reported previously that PEG drives model membrane bilayers to within molecular contact and, in the process, extracts water from the trapped vesicle compartment thereby flattening and perhaps destabilizing the vesicles (Burgess *et al.*, 1992). This combination of surface and interior dehydration can leave the vesicle intact, can result in vesicle rupture, or can result in vesicle fusion when bilayer membranes are appropriately perturbed (Lentz *et al.*, 1992; Massenburg & Lentz, 1993). While bilayer perturbation is essential, it appears that interior dehydration is not required for fusion (Lentz *et al.*, 1997), nor is vesicle rupture, which often accompanies fusion but is a mechanistically distinct process (Massenburg & Lentz, 1993; Lentz *et al.*, 1997). Fusogenic bilayer perturbation may result from certain amphipathic impurities, high membrane curvature, or packing disruption in the bilayer outer leaflet (Lentz *et al.*, 1992, 1996; Wu *et al.*, 1996; Lee & Lentz, 1997). Although we have shown that two fusing vesicle systems share a common outer leaflet structural perturbation, it remains a challenge to define the essential bilayer structural perturbations that lead to fusion of PEG-aggregated membranes (Lentz, 1994).

The experiments reported here were stimulated by a report of PEG-induced fusion between small, unilamellar vesicles (SUV) composed of hen egg yolk phosphatidylcholine (PC;

† Supported by USPHS Grant GM32707.

* To whom requests for reprints should be addressed. E-mail: UNCBRL@MED.UNC.EDU.

⊗ Abstract published in *Advance ACS Abstracts,* May 1, 1997.

[1] Abbreviations: PEG, poly(ethylene glycol); ANTS, 8-aminonaphthalene-1,3,6-trisulfonic acid, disodium salt; DPX, *N*,*N*′-*p*-xylenebis(pyridinium bromide); TES, *N*-[tris(hydroxymethyl)methyl]-2-aminoethanesulfonic acid; $C_{12}E_8$, dodecyloctaethylene glycol monoether; PC, phosphatidylcholine; DMPC, 1,2-dimyristoyl-3-*sn*-phosphatidylcholine; DPPC, 1,2-dipalmitoyl-3-*sn*-phosphatidylcholine; DOPC, 1,2-dioleoyl-3-*sn*-phosphatidylcholine; DLPC, 1,2-dilinolenoyl-3-*sn*-phosphatidylcholine; POPC, 1-palmitoyl-2-oleoyl-3-*sn*-phosphatidylcholine; egg PC, hen egg yolk phosphatidylcholine; PAPC, 1-palmitoyl-2-arachidonoyl-3-*sn*-phosphatidylcholine; PLPC, 1-palmitoyl-2-linoleoyl-3-*sn*-phosphatidylcholine; DPA, pyridine-2,6-dicarboxylic acid; cholic acid, 3α,7α,12α-trihydroxy-5β-cholan-24-oic acid; SUVs, small unilamellar vesicles; LUVs, large unilamellar vesicles; C_6-NBD-PC, 1-palmitoyl-2-*N*-(4-nitrobenzo-2-oxa-1,3-diazole)aminohexanoylphosphatidylcholine; TMA-DPH, 1-(4-trimethylammonium)-6-phenyl-1,3,5-hexatriene; DPHpPC, 1-palmitoyl-2-[[2-[4-(6-phenyl-*trans*-1,3,5-hexatrienyl)phenyl]ethyl]carboxyl]-3-*sn*-phosphatidylcholine.

S0006-2960(96)02437-3 CCC: $14.00

Viguera *et al.*, 1993). The report of SUV fusion at high PEG concentrations appeared to contradict our observation of rupture of such highly curved membranes (Lentz *et al.*, 1992). To complicate matters, this report detected vesicle fusion using an assay for the mixing of membrane contents that had not been applied previously to PEG-mediated fusion. This assay (Wilschut *et al.*, 1980) monitors the enhanced fluorescence of Tb^{3+} trapped in one membrane compartment when it is mixed with dipicolinic acid (DPA) encapsulated in a second membrane compartment. Viguera *et al.* (1993) performed this assay in the presence of high concentrations of PEG but did not report assay details. Since our studies had shown how sensitive to misinterpretation are fluorescence assays performed even in the presence of low concentrations of PEG (Lentz *et al.*, 1992), we set out to confirm and expand upon the result reported by Viguera *et al.* (1993).

Several significant conclusions are derived from this effort. First, we have confirmed that the Tb^{3+}/DPA assay can be performed in the presence of PEG, and we document here how to do so. Second, we have demonstrated what we have previously only been able to suggest based on interpretation of data documenting the intermixing of lipids between apposed membranes (Wu & Lentz, 1994), namely, that fusion occurs in the dehydrated state between vesicles aggregated by PEG. Third, we have confirmed that membrane curvature is one factor that favors fusion of phospholipid vesicles aggregated in the presence of PEG. Fourth, we have found that the apparent discrepancy between the observations of Viguera *et al.* (1993) and our observations (Lentz *et al.*, 1992) was due to the fact that PC species with unsaturated acyl chains favor PEG-mediated fusion. Finally, we have shown that the combined effect of high curvature and acyl chain unsaturation is to increase the rate of lipid motions and decrease lipid order in the upper regions of SUV bilayer outer leaflets. These effects correlated inversely with the concentration of PEG needed to promote fusion.

MATERIALS

Chloroform stock solutions of hen egg yolk L-α-phosphatidylcholine (egg PC), 1,2-dimyristoyl-3-*sn*-phosphatidylcholine (DMPC), 1,2-dipalmitoyl-3-*sn*-phosphatidylcholine (DPPC), 1-palmitoyl-2-oleoyl-3-*sn*-phosphatidylcholine (POPC[1]), 1-palmitoyl-2-linoleoyl-3-*sn*-phosphatidylcholine (PLPC), 1-palmitoyl-2-arachidonoyl-3-*sn*-phosphatidylcholine (PAPC), 1,2-dilinolenoyl-3-*sn*-phosphatidylcholine (DLPC), 1,2-dioleoyl-3-*sn*-phosphatidylcholine (DOPC), and 1-palmitoyl-2-*N*-(4-nitrobenzo-2-oxa-1,3-diazole)aminohexanoylphosphatidylcholine (C_6-NBD-PC) were purchased from Avanti Polar Lipids, Inc. (Birmingham, AL) and used without further purification. Dodecyl octaethylene glycol monoether ($C_{12}E_8$) was purchased from Calbiochem (LaJolla,CA). 3α,7α,12α-Trihydroxy-5β-cholan-24-oic acid (cholic acid), L-histidine, pyridine-2,6-dicarboxylic acid (DPA), and *N*-[tris(hydroxymethyl)methyl]-2-aminoethanesulfonic acid (TES) were purchased from Sigma Chemical Co. (St. Louis, MO). Terbium chloride was purchased from Johnson Matthey Co. (Ward Hill, MA). The disodium salt of 8-aminonaphthalene-1,3,6-trisulfonic acid (ANTS), *N*-*N*′-*p*-xylylenebis(pyridinium bromide) (DPX), 1,6-diphenyl-1,3,5-hexatriene (DPH), and 1-(4-trimethylammonium)-6-phenyl-1,3,5-hexatriene (TMA-DPH) were purchased from Molecular Probes (Eugene, OR). Carbowax PEG 8000 (molecular weight 7000−9000) was purchased from Fisher Scientific (Fairlawn, NJ) and purified as described previously (Parente & Lentz, 1986; Lentz *et al.*, 1992). All other reagents were of the highest quality available.

METHODS

Vesicle Preparation. Large unilamellar vesicles (LUV) were prepared by the high-pressure extrusion method. Appropriate quantities of chloroform stocks of phospholipid were dried under a stream of nitrogen. The dried lipid was dissolved in cyclohexane, frozen, dried under vacuum overnight to produce a white powder, and suspended in the appropriate assay buffer above the lipid order/disorder phase transition. For the ANTS/DPX contents mixing assay, lipids were suspended in buffer containing either 25 mM ANTS plus 40 mM NaCl or 90 mM DPX, and 10 mM TES, pH 7.4. Vesicles for ANTS/DPX leakage experiments were prepared in a buffer containing 12.5 mM ANTS, 45 mM DPX, 20 mM NaCl, and 10 mM TES, pH 7.4. For the Tb/DPA contents mixing measurements, lipid was suspended in either 150 mM DPA or 15 mM $TbCl_3$ plus 150 mM sodium citrate, and 2 mM TES/2 mM L-histidine, pH 7.4. Tb/DPA leakage experiments employed vesicles prepared in buffer containing 7.5 mM $TbCl_3$, 75 mM sodium citrate, 75 mM DPA, 2 mM TES, and 2 mM L-His. In all cases, multilamellar vesicles resulting from suspending lipids in these different buffers were extruded seven times through a 0.1-μm polycarbonate filter under a pressure of about 75 psi of argon to generate LUV (Mayer *et al.*, 1986).

Small unilamellar vesicles (SUV) were prepared by subjecting multilamellar vesicle suspensions to sonic disruption in a Heat Systems Model 350 sonicator (Plainview, NY). SUV preparations were fractionated by centrifugation at 70 000 rpm for 25 min (4 °C for egg PC and other unsaturated PCs, 28 °C for DMPC, and 40 °C for DPPC in a rotor preheated to 50 °C) in a Beckman TL-100 ultracentrifuge (Palo Alto, CA). SUVs were maintained above their phase transition at all times and used within 1 h of centrifugation. All measurements on SUVs were performed at temperatures above their phase transitions (room temperature for unsaturated lipids, 28 °C for DMPC, and 45 °C for DPPC). Average vesicle diameters were determined by quasi-elastic light scattering (Lentz *et al.*, 1992) to be 38 nm for SUVs and 135 nm for LUVs, although size varied considerably with lipid composition.

ANTS/DPX Leakage and Contents Mixing. The ANTS/DPX contents mixing and leakage assays were based upon those originally proposed by Ellens *et al.* (1984) and applied to PEG-mediated vesicle fusion as previously described (Lentz *et al.*, 1992). Because fluorescent impurities in PEG contribute significantly in the spectral range of maximal ANTS fluorescence, vesicle samples (0.4 mL) were diluted following incubation (5 min) with PEG to a final volume of 3.5 mL before recording ANTS fluorescence and PEG background intensity (Lentz *et al.*, 1992). Leakage experiments used vesicles (0.5 mM lipid in the assay sample) in which equimolar ANTS and DPX were co-encapsulated, such that DPX quenched at least 85% of the ANTS fluorescence. When leakage of contents occurred, there was an increase in fluorescence due to the dilution of ANTS and DPX into the extravesicular compartment. The fluorescence intensity of a co-encapsulated ANTS/DPX vesicle sample plus the background intensity contributed by PEG was taken as characteristic of 0% leakage. Similarly, 100% leakage was

characterized by the PEG background plus the fluorescence intensity of an ANTS/DPX vesicle sample to which detergent ($C_{12}E_8$ at 0.46 mM final concentration) had been added to release vesicle contents. Contents mixing assays were carried out by adding equal volumes of ANTS-containing and DPX-containing vesicles to buffer (each to a final concentration of 0.25 mM lipid) at a specified PEG concentration. After incubation, the sample was diluted 8.8-fold with buffer, and ANTS fluorescence was recorded. The fluorescence intensity of ANTS-containing vesicles in PEG was taken to represent 0% contents mixing. As described previously (Lentz *et al.*, 1992), calculation of "percent contents mixing" was based on the assumption of one "ideal round" of fusion, *i.e.*, fusion occurring between pairs of aggregated vesicles. Thus, 100% contents mixing was represented by the fluorescence intensity of co-encapsulated ANTS/DPX vesicles plus PEG. The calculations leading to reported values of percent contents mixing accounted for the leakage of contents, for the photobleaching of ANTS, and also for the probability that two fusing vesicles contained ANTS and DPX (Lentz *et al*., 1992). Since fusion likely occurs in aggregates larger than dimers (Wu & Lentz, 1994), this will underestimate the actual percentage of vesicles that have experienced fusion events.

Tb/DPA Leakage and Contents Mixing. The Tb/DPA contents mixing and leakage assays were based on assays previously described (Wilschut *et al*., 1980) except that the concentration of lipid used was 0.7 mM and the measurements were carried out in a final buffer concentration of 185 mM NaCl, 3.7 mM L-His, 3.7 mM TES, 2.0 mM EDTA, and 20 mM $CaCl_2$, pH 7.4. The major differences between this assay and the ANTS/DPX assay are, first, that the fluorescence of Tb^{3+} complexed with DPA does not overlap with that of the fluorescent impurity in PEG, and, second, that the change in fluorescence associated with fusion is greater for the Tb^{3+}/DPA than for the ANTS/DPX assays. Thus, Tb^{3+} fluorescence could be monitored in the presence of PEG. When leakage of contents occurred, there was a drop in fluorescence due to the quenching by water (Horrocks & Sudnick, 1979) of Tb^{3+} released from complexation with DPA due to dilution of the trapped compartment into the external compartment. As for the ANTS/DPX assay (Lentz *et al.*, 1992), 0% leakage was assumed to be defined by the fluorescence intensity of the co-encapsulated Tb/DPA vesicles in buffer without PEG ($F_{co}^{0\%}$). The fluorescence intensity of Tb/DPA vesicles treated with detergent (11.6 mM sodium cholate) was taken as representing 100% leakage of trapped contents, in the absence ($F_{co}^{0\%,det}$) or presence ($F_{co}^{x\%,det}$) of PEG. With these definitions and the same assumptions made in quantitating the ANTS/DPX assay

$$\%\ \text{leakage} = \frac{(F_{co}^{0\%} - F_{co}^{0\%,det}) - (F_{co}^{x\%} - F_{co}^{x\%,det})}{(F_{co}^{0\%} - F_{co}^{0\%,det})} \quad (1)$$

LUVs showed the same amount of leakage at low (0.07 mM) as at high (0.7 mM) vesicle concentration, eliminating the possibility that light scattering distorted the measurement of leakage.

Contents mixing assays were carried out by incubating equal volumes of separate vesicle populations (each at a final lipid concentration of 0.35 mM) containing Tb^{3+} and DPA, respectively, with buffer containing *x*% PEG. After 5 min of incubation, the fluorescence intensity was read ($F_{sep}^{x\%}$), detergent was added to release the contents of the vesicles, and fluorescence intensity was again recorded ($F_{sep}^{x\%,det}$). All measurements were made without dilution. Again, assuming that one ideal round of fusion involves mixing of contents between aggregated pairs of vesicles, the percent of ideal contents mixing can be calculated as

$$\%\ \text{contents mixing} = \frac{(F_{sep}^{x\%} - F_{sep}^{x\%,det})}{1/2(F_{co}^{x\%} - F_{co}^{x\%,det})} \quad (2)$$

This equation corrects for the fact that fusing vesicles that have leaked some of their contents will register a smaller fluorescence change (*i.e.*, $F_{co}^{x\%}$ will already be reduced relative to $F_{co}^{0\%}$ due to contents loss) and for the probability (1/2) that two fusing vesicles contain Tb^{3+} in one and DPA in the other. Because the correction for leakage effectively magnifies a small signal, both the ANTS/DPX and the Tb^{3+}/DPA assays are less accurate under conditions of extreme leakage. As for the ANTS/DPX assay, the Tb^{3+}/DPA assay probably underestimates the fraction of vesicles experiencing a fusion event (see above).

Phase-Resolved Fluorescence Measurements with TMA-DPH and C_6-NBD-PC. TMA-DPH measurements were made using the SLM-48000MHF spectrofluorometer with excitation in a region from 351.1 to 363.8 nm of the laser UV wavelengths of a Coherent Innova 90-4 laser (Auburn, CA) using a correlation frequency of 60 Hz and 300 data averaging. A base modulation frequency of 4 MHz was used with data collected at 37 frequencies geometrically related to this base frequency (4−148 MHz). Small alloquotes (ca. 1−2 μL) of probe stock solutions (DPH in acetone, TMA-DPH in methanol) were added to preformed vesicle suspensions and allowed to equilibrate to constant fluorescence intensity before making lifetime measurements. The lipid:probe ratio and lipid concentration used were 250−300:1 and 0.2 mM, respectively. All lifetime measurements were obtained with glycogen as a reference. For lifetime measurements, the polarizer in the emission channel was set at the magic angle (37.5° from vertical). Phase-resolved dynamic anisotropy measurements were performed using the T format with the excitation polarizer vertical. Phase shift and modulation ratio values were analyzed to obtain lifetimes, and differential polarized phase shift and modulation ratios were analyzed to characterize TMA-DPH motion using the Globals Unlimited software package developed at the Laboratory for Fluorescence Dynamics, Department of Physics, University of Illinois (Urbana, IL) as described elsewhere (Lentz *et al.*, 1996).

C_6-NBD-PC was excited with the Coherent Inova 90-4 argon-ion laser at a wavelength of 488 nm, and emission was detected through a 2-mm OG-515 filter. In the presence of membranes, C_6-NBD-PC partitions between the membrane and a micellar phase (Lee & Lentz, 1997). Lifetimes and mole fractions of probe in a membrane and in a micelle environment were estimated using phase-resolved lifetime analysis employing the Globals Unlimited software package as described in detail elsewhere (Lee & Lentz, 1997).

RESULTS

PEG-Mediated Vesicle Fusion Can Be Characterized Using the Tb/DPA Assay. In our earliest attempt to characterize PEG-mediated model membrane fusion (Parente & Lentz, 1986), we abandoned the Tb/DPA assay system

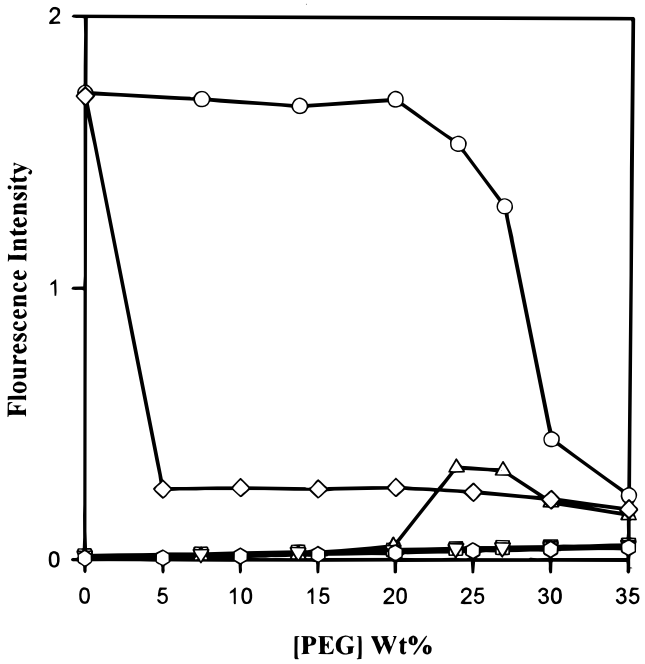

FIGURE 1: PEG-induced changes in Tb^{3+} fluorescence for egg PC SUVs using the Tb/DPA assay. Shown are data for co-encapsulated Tb/DPA vesicles in the absence (circles) and presence (squares) of 11.6 mM sodium cholate and for mixtures of separate Tb^{3+} and DPA-containing vesicles in the absence (triangles) and presence (inverted triangles) of sodium cholate detergent. Measurements were carried out using 0.7 mM lipid in the Tb/DPA fusion buffer (see Methods). Also shown is the fluorescence intensity from 3.15 μM Tb^{3+} and 31.5 μM DPA (concentrations estimated to be released from lysed co-encapsulated or mixed vesicles) in Tb/DPA fusion buffer with (open hexagons) and without (diamonds) EDTA and $CaCl_2$.

because of the observed quenching of the Tb/DPA complex fluorescence by PEG. The report of Viguera *et al.* (1993) encouraged us to re-evaluate the potential of this assay system to report PEG-mediated fusion. Figure 1 displays the fluorescence of the Tb/DPA complex encapsulated in vesicles (open circles) and free in solution (open diamonds) at the same "total cuvette concentration". It is evident from the result in the absence of PEG that encapsulation was not necessary for formation of a fluorescent Tb/DPA complex. Thus, release of the Tb/DPA complex was not sufficient to cause quenching of Tb^{3+} fluorescence (compare open diamonds with circles in Figure 1), in agreement with the original report of Wilschut *et al.* (1980). These authors noted that optimal quenching of released Tb^{3+} required the presence of Ca^{2+} and Na_2EDTA, apparently to force the release of Tb^{3+} from its complex with DPA. The presence of these components in the buffer with unencapsulated Tb/DPA caused nearly complete loss of Tb^{3+} fluorescence, in the absence and presence of PEG (hexagons in Figure 1).

The data in Figure 1 also demonstrate that the unencapsulated Tb/DPA complex is indeed quenched by PEG, while encapsulated complex is unaffected by PEG (constancy of the open circles up to 20 wt % PEG). Note that the slight rise in the signal with PEG concentration in the presence of detergent (squares and inverted triangles) was due to PEG alone, since it was the same in the absence of lipid and detergent (hexagons in Figure 1). The lack of an effect of PEG on encapsulated Tb/DPA or on free Tb/DPA (in the presence of Ca^{2+} plus Na_2EDTA) confirms the ability of this complex to monitor PEG-mediated fusion.

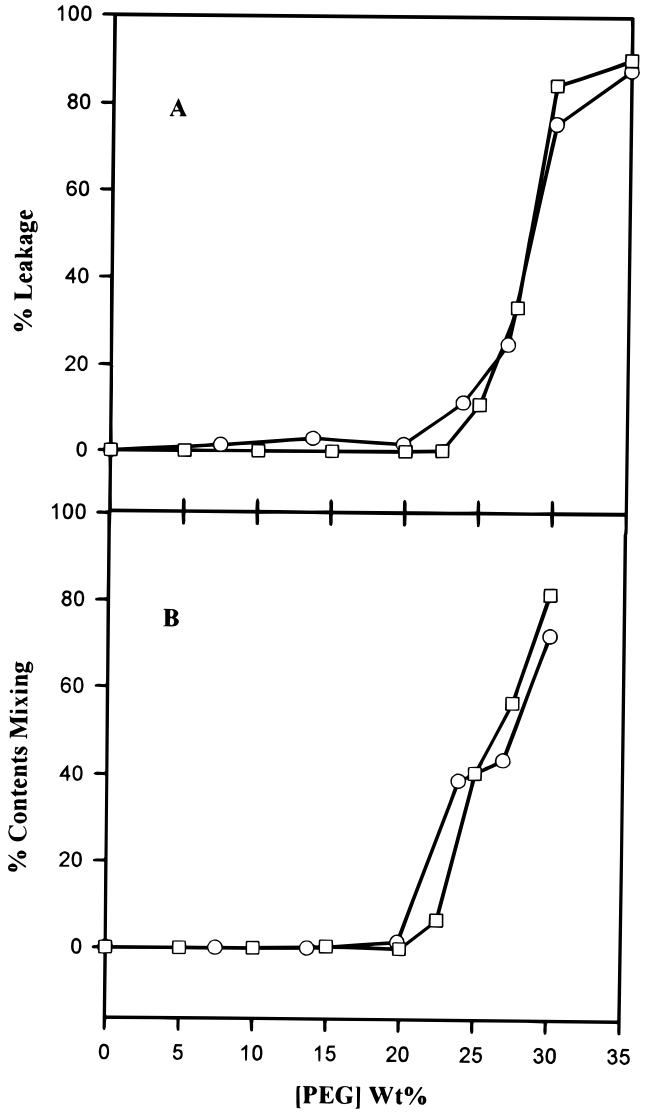

FIGURE 2: PEG-induced leakage and contents mixing of egg PC SUV. Vesicle leakage (A) and contents mixing (B) were monitored as a function of PEG concentration using the ANTS/DPX assay (squares) and the Tb/DPA assay (circles). Tb/DPA assay measurements were carried out as described in Figure 1 and in Methods. ANTS/DPX assay measurements were performed with 0.5 mM lipid in 100 mM NaCl, 2 mM TES, and 1 mM EDTA, pH 7.4; vesicles were diluted to 0.057 mM lipid in the same buffer for measurement (see Methods).

To illustrate further the Tb/DPA assay as applied to monitoring fusion, we have recorded in Figure 1 the four fluorescence measurements needed for quantitating fusion and leakage according to eqs 1 and 2: (1) $F_{co}^{x\%}$ (open circles); (2) $F_{co}^{x\%,det}$ (open squares); (3) $F_{sep}^{x\%}$ (open triangles); and $F_{sep}^{x\%,det}$ (open inverted triangles). It is clear from these data that, even in the presence of high concentrations of PEG, the Tb/DPA complex appears capable of reporting either contents leakage (circles and squares) or contents mixing (triangles and inverted triangles). To confirm this, we have compared in Figure 2 the results of contents leakage (A) and contents mixing (B) assays performed on egg PC SUVs using the Tb/DPA (circles) and ANTS/DPX (squares) assays. The results are nearly identical, thereby confirming the validity of both assays. Of special note is the fact that the Tb/DPA assay, unlike the ANTS/DPX assay, reported fusion of this vesicle system in the presence of PEG. This confirms our earlier conclusion, based on lipid exchange measurements, that fusion occurs

between contacting vesicles aggregated by PEG rather than requiring the osmotic stress that might be associated with dilution of PEG (Wu & Lentz, 1994).

Chain Unsaturation and High Curvature Favor PEG-Mediated Fusion. It has long been known that saturated PC SUVs fuse readily below (Surrkuusk *et al.*, 1976; Schullery *et al.*, 1980) and even slowly above the order/disorder phase transition (Lentz *et al.*, 1987). We have reported previously that bilayer curvature increases the probability of fusion between DPPC vesicles aggregated by PEG (Lentz *et al.*, 1992). However, LUVs with diameters smaller than 700 Å and, in particular, SUVs were found to rupture rather than fuse in the presence of high concentrations of PEG (Lentz *et al.*, 1992). The report of PEG-mediated fusion of egg PC SUVs (Viguera *et al.*, 1993) required that we re-address the issue of whether extreme curvature enhanced osmotic fragility or fusion, or both.

The data in Figure 2 confirm, both qualitatively and quantitatively, the report of Viguera *et al.* (1993) that PEG induces fusion of egg PC SUVs at a concentration for which leakage is minimal. Using the ANTS/DPX assay, we had shown that leakage of contents from DPPC SUVs began at PEG concentrations of 10−15 wt %, while no contents mixing was observed up to 35 wt % PEG (Lentz *et al.*, 1992). Since the ANTS/DPX assay requires dilution of PEG before making fluorescence measurements, we repeated our experiments on DPPC SUVs using the Tb/DPA assay. The results are presented in Figure 3. The results confirm the essential results obtained with the ANTS/DPX assay, indicating that PEG causes DPPC SUVs to rupture before they fuse, even in the dehydrated state. We have already reported that DPPC LUVs were not induced to fuse by PEG concentrations up to 35 wt %, although they did rupture at concentrations at and above 30 wt % (Burgess *et al.*, 1991).

We ask next whether there is any correlation between the extent of acyl chain unsaturation in a PC species and the ability of this species to form vesicles that can be fused by PEG. To answer this question, we present in Figure 4, panels A and B, a summary of the effect of PEG on SUVs prepared from six PC species of varying degrees of unsaturation. Examination of these data reveals a clear correlation between chain unsaturation and both the extent of fusion (maximum extent of contents mixing) and the ease of fusion (minimum PEG concentration needed to induce fusion). We note also that SUVs produced from these doubly unsaturated PCs generally fused at PEG concentrations lower than those needed to cause rupture.

Is the ability of PEG to fuse SUVs a reflection only of the unsaturation of the PC species present in the SUVs, or does SUV bilayer curvature contribute to the ability to fuse? In order to answer this question, we monitored the effect of PEG on LUVs prepared from egg PC or POPC. The results are summarized in Figure 5, panels A and B, respectively. As for DPPC LUVs, PEG induced rupture at high PEG concentrations. Egg PC LUVs, however, were induced to fuse at 35 wt % PEG, but only to a small extent. POPC LUVs, being somewhat less unsaturated than egg PC LUV, did not fuse at PEG concentrations up to 35 wt %. Apparently, the ability of egg PC and POPC SUVs to fuse at 22.5 and 27.5 wt % PEG depends both on these lipid's unsaturated acyl chains and on the extreme curvature of SUVs. Chain unsaturation and SUV curvature seem also to be linked parameters. Thus, curvature (1/radius) increases in proportion to increased chain unsaturation for both doubly

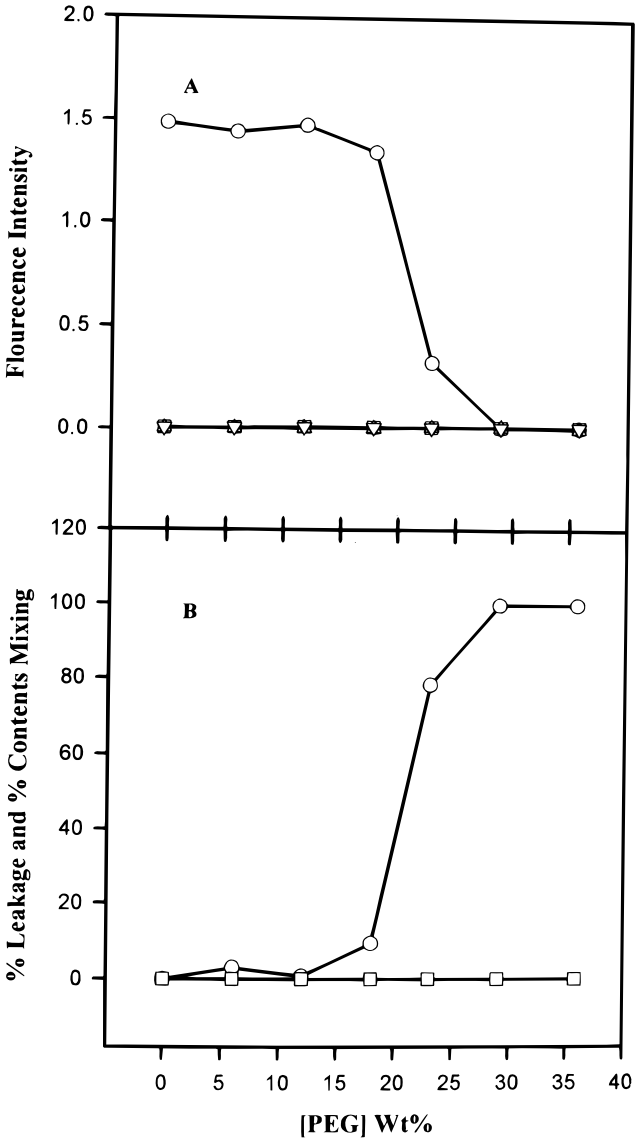

FIGURE 3: PEG-induced fusion of DPPC SUVs using the Tb/DPA assay. (A) Changes in Tb^{3+} fluorescence are shown as a function of PEG concentration for co-encapsulated vesicles in the absence (circles) and presence of 11.6 mM sodium cholate (squares), mixtures of separate Tb^{3+} and DPA-containing vesicles in the absence (triangles) and presence (inverted triangles) of cholate. (B) Data from A were used to calculate PEG-induced percent contents mixing (squares) and percent leakage (circles).

unsaturated and mixed-chain PCs, although the two types of lipids appear to display somewhat different behaviors (Figure 7A). Because the concentration of PEG needed to mediate fusion decreases with increasing chain unsaturation, there is a clear correlation between chain unsaturation and fusogenicity (Figure 8A).

Because curvature and chain unsaturation are somewhat differently correlated in the two types of lipid species examined, these two types of SUVs may have somewhat different bilayer structural features. We ask now what feature(s) of unsaturated SUV bilayers might make them susceptible to PEG-mediated fusion. Chain unsaturation decreases the chain melting temperature and is expected, at a given temperature, to increase the interfacial area per lipid molecule (Rand & Parsegian, 1989). This might be expected to exacerbate the packing problem already experienced by the outer leaflet of SUV bilayers, allowing more water penetration and creating an even more unstable interface with the water phase. We have previously reported that increased

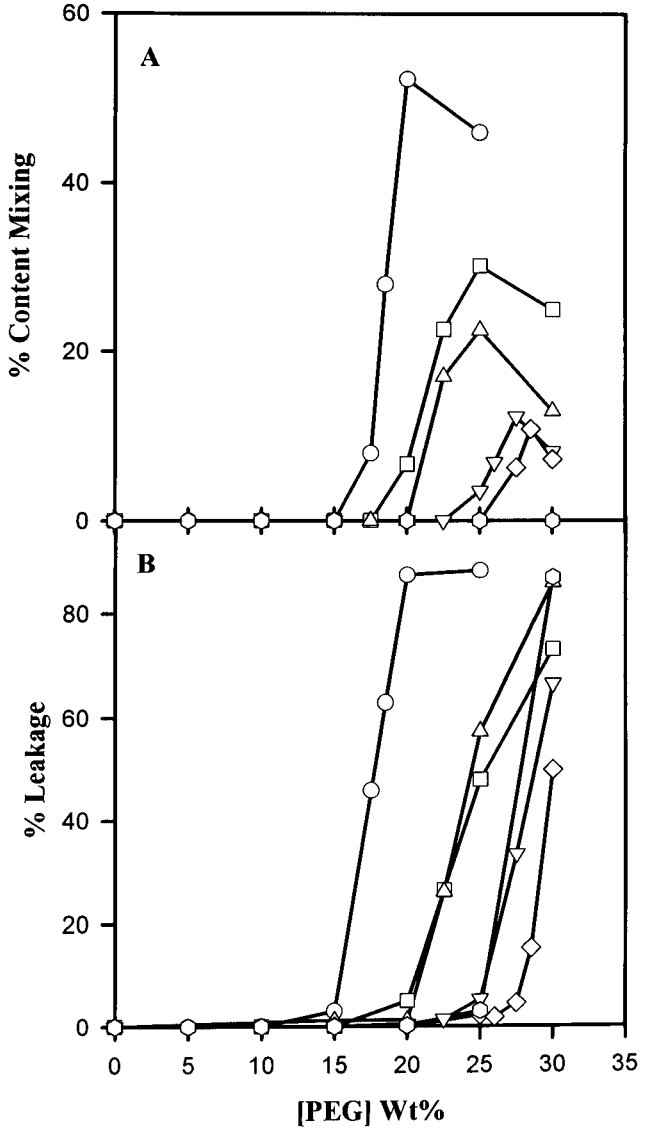

FIGURE 4: PEG-induced fusion of SUVs containing unsaturated phosphatidylcholines. PEG-induced contents mixing (A) and leakage (B) of SUVs composed of DMPC (hexagons), POPC (diamonds), PAPC (triangles), PLPC (inverted triangles), DOPC (squares), and DLPC (circles). Experiments were carried out using 0.057 mM lipid in the presence of the indicated concentrations of PEG. Content mixing was measured by the Tb/DPA assay, and leakage was measured by the ANTS/DPX assay.

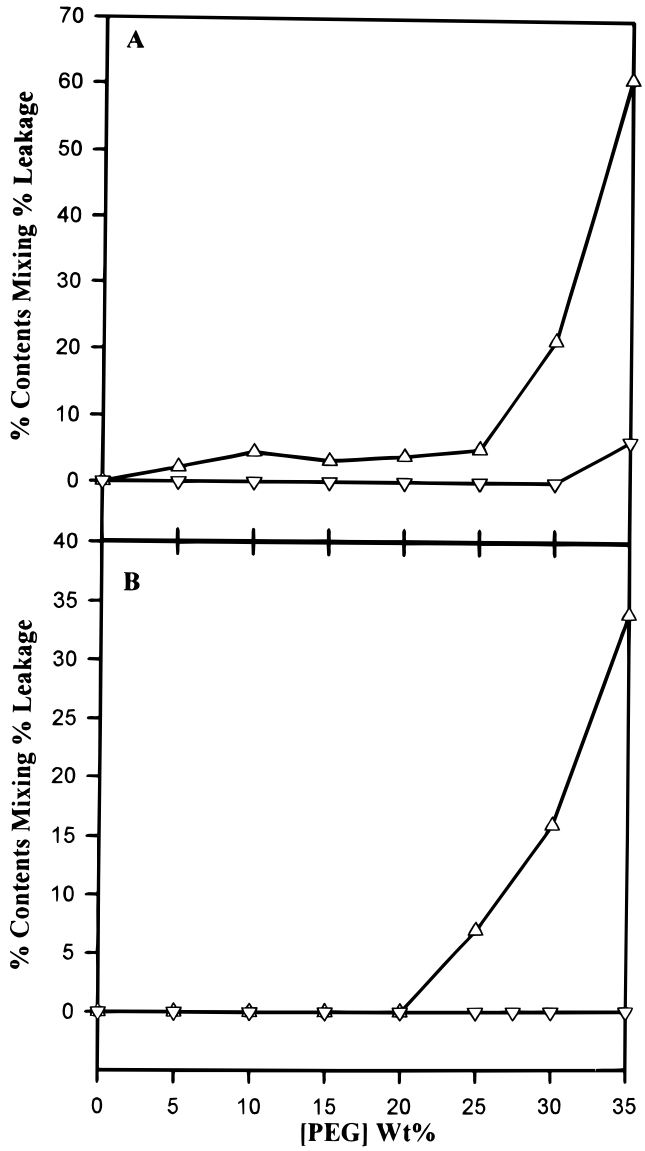

FIGURE 5: PEG-induced fusion of LUV. PEG-induced leakage (triangles) and contents mixing (inverted triangles) of (A) egg PC and (B) POPC LUV. Measurements used 0.5 mM lipid and the ANTS/DPX assay.

rates of thermal motions and decreased lipid packing density in contacting bilayer leaflets were necessary for PEG-mediated fusion (Lee & Lentz, 1997). We report next our efforts to use two fluorescent amphipaths, C_6-NBD-PC and TMA-DPH, to probe the outer leaflets of the unsaturated SUV bilayers examined here.

Behavior of C_6-NBD-PC in Highly Curved, Unsaturated Membranes. We show elsewhere that LUVs whose membrane outer leaflets have been perturbed by lipid removal or by lipid shape changes demonstrate an enhanced ability to incorporate C_6-NBD-PC from micelles and enhance the quantum yield of this probe (Lee & Lentz, 1997). These changes in C_6-NBD-PC properties correlated with increased fusogenicity. We asked whether there would be a similar correlation in the unsaturated SUV series examined here. The results of these experiments presented as a function of lipid/probe ratio are presented in Figure 6. With the exception of one point at 750 lipids/probe, the lifetime of membrane-associated C_6-NBD-PC was essentially invariant while the fraction of probe in the bilayer increased with increasing lipid/probe ratio. It is clear that C_6-NBD-PC partitioned less favorably into and had a lower quantum yield in fusogenic unsaturated bilayers than into the non-fusing, saturated DMPC bilayers (octagons) to which we compared these. This is opposite to what was observed in the fusogenic, perturbed LUV membranes that we studied previously (Lee & Lentz, 1997). In Figures 7 and 8, we summarize the variation of C_6-NBD-PC properties at a single lipid/probe ratio (500) with the degree of unsaturation of the lipids used (Figure 7) and then with the fusogenicity of SUV preparations (Figure 8). It is clearly seen that the behavior of the probe was different in SUVs prepared from doubly unsaturated versus mixed-chain (saturated/unsaturated) phospholipids. For the latter class of lipids, both the fluorescent lifetime and the fraction of probe associated with the membrane decreased with increasing unsaturation (circles in Figure 7, panels D and E). For doubly unsaturated PCs, however, the fraction of membrane-associated probe increased slightly with unsaturation (circles), while the lifetime of C_6-NBD-PC was unaffected by the number of acyl chain double bonds (squares). For both types of lipids, increased chain unsat-

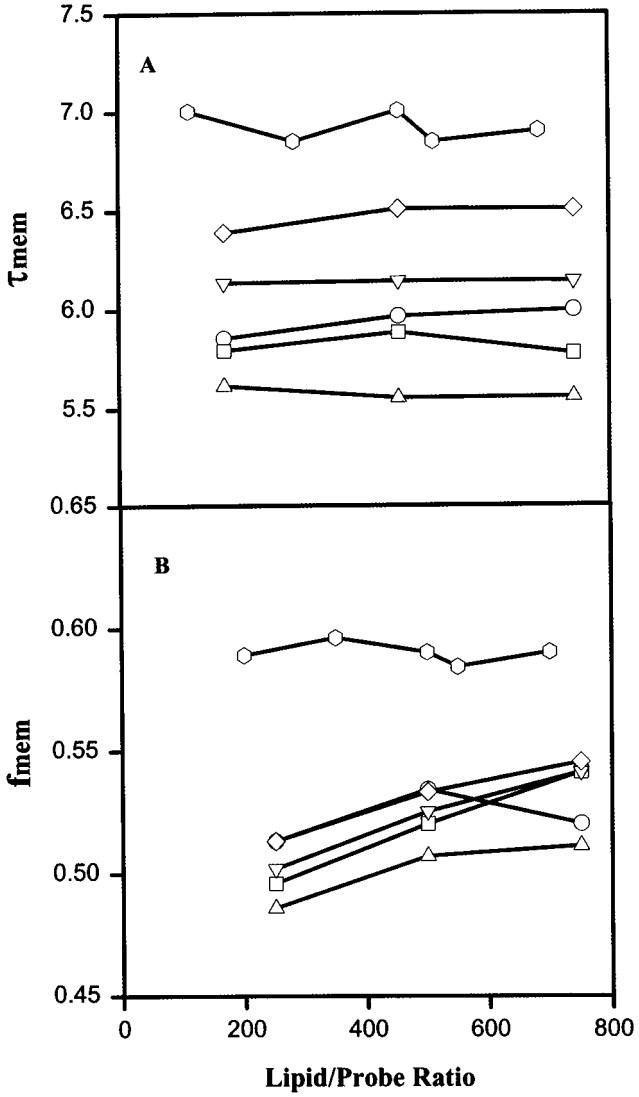

FIGURE 6: Behavior of C_6-NBD-PC in various SUV preparations. The average lifetime (τ_{mem}) of membrane-associated C_6-NBD-PC (A) and the mole fraction (f_{mem}) of C_6-NBD-PC associated with the membrane (B) are displayed over a range of lipid/probe ratios for the SUV preparations examined here. Symbols indicating lipid species are as in Figure 4.

uration increased SUV fusogenicity [*i.e.*, decreased the PEG concentration needed to mediate fusion (Figure 4)]. Consistent with this, the behavior of C_6-NBD-PC did not uniformly correlate with fusogenicity (Figure 8D). The ability of C_6-NBD-PC to partition into a membrane correlated directly with fusogenicity only for the two doubly unsaturated lipids we studied, while the opposite behavior was seen for SUVs prepared from mixed-chain lipids (Figure 8D).

Behavior of TMA-DPH in Highly Curved, Unsaturated Membranes. Ho *et al.* (1995) have used the excited-state lifetime of a chain-labeled phosphatidylcholine (DPHpPC) to suggest a correlation between water penetration and decreased membrane order associated with increased chain unsaturation in LUV. We have used the excited-state lifetime of a similar molecule, TMA-DPH, to monitor the polarity in the upper regions of bilayers (Lee & Lentz, 1997) composed of PCs of different acyl chain unsaturation. TMA-DPH has an advantage over DPHpPC in that it can be added directly and exclusively to the outer leaflets of preformed vesicles. The outer leaflets of PEG-aggregated vesicles come into contact during PEG-mediated fusion and are, thus, the focus of our attention. TMA-DPH, on the other hand, has

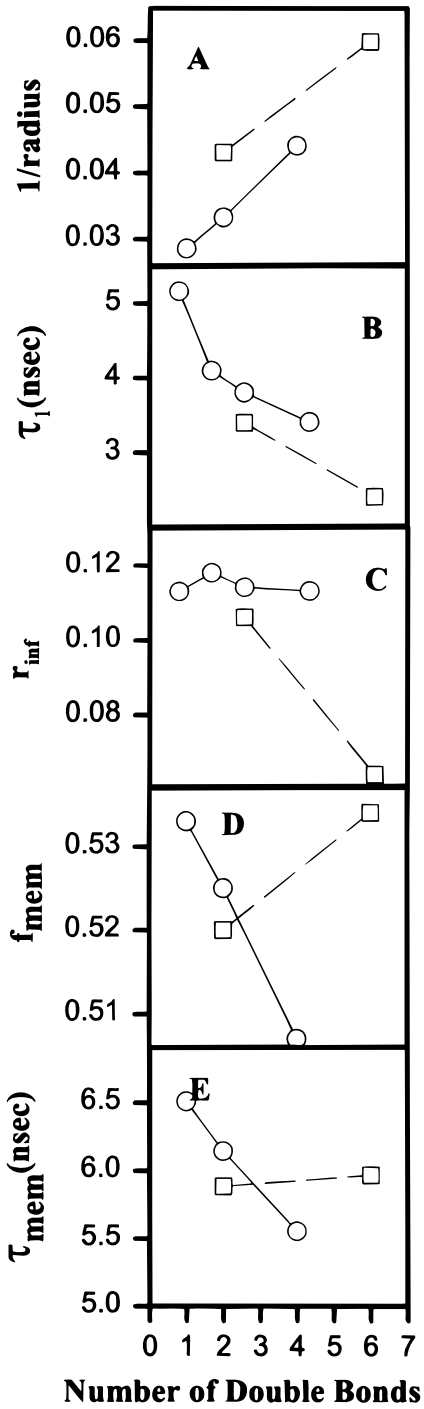

FIGURE 7: Vesicle curvature and the behavior of TMA-DPH and C_6-NBD-PC in phosphatidylcholine SUVs as a function of chain unsaturation. (A) SUV curvatures (1/radius) were calculated from mean hydrodynamic radii measured by QELS and are plotted versus the number of unsaturated chains for lipids containing unsaturated chains in both the *sn*-1 and *sn*-2 positions (squares) or an unsaturated chain in only the *sn*-2 position of glycerol (circles). (B and C) TMA-DPH fluorescence lifetime measurements were performed at room temperature as described in Methods at a lipid/probe ratio of 300:1. For each lipid, two lifetime components were obtained by Globals Unlimited and are given in Table 1. The larger lifetime component (τ_1) and the limiting anisotropy (R_{inf}) are plotted in B and C, respectively. (D and E) The mole fractions (f_{mem}) of C_6-NBD-PC associated with the membrane and the average lifetimes (τ_{mem}) of membrane-associated C_6-NBD-PC at a lipid/probe ratio of 500 are plotted in D and E, respectively.

a small disadvantage relative to DPHpPC in that it is expected to be slightly more variable in its vertical position, relative to the water/hydrocarbon interface, than is DPHpPC (Stubbs *et al.*, 1995).

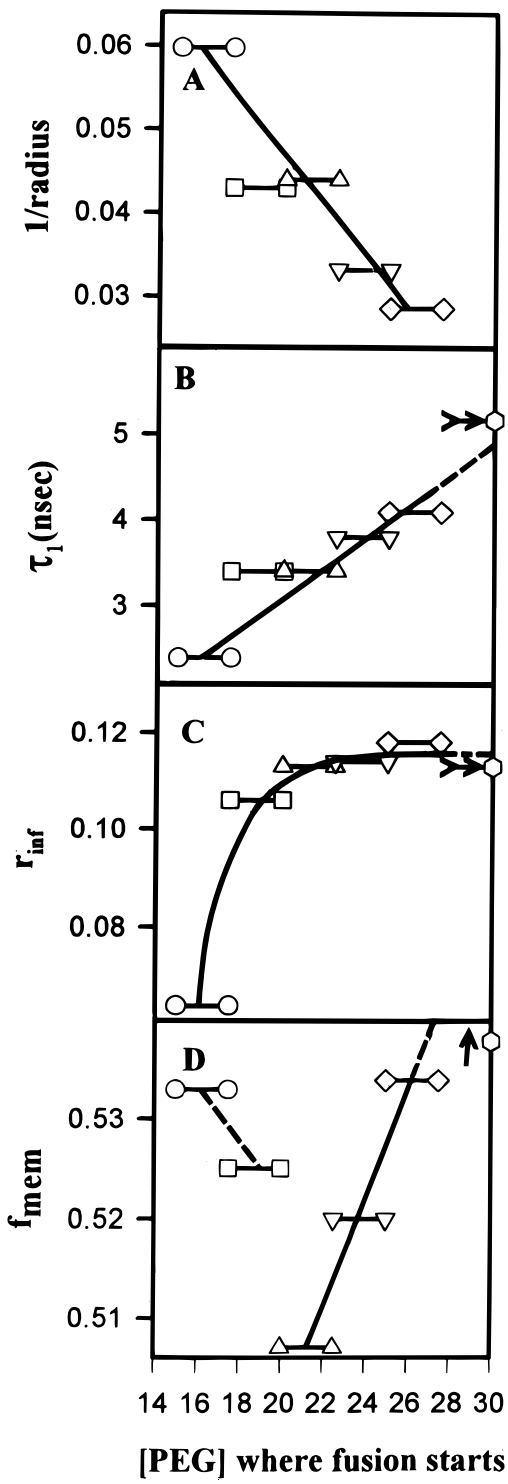

FIGURE 8: SUV structural properties as a function of PEG concentrations needed to induce vesicle fusion. (A) SUV curvatures (see Figure 7A) are plotted as a function of the range of PEG concentration in which fusion was first detected by our contents mixing assays (see Figure 4). (B and C) TMA-DPH fluorescence lifetime (τ_1) and limiting anisotropy (R_{inf}), respectively, are similarly plotted. (D) The mole fractions (f_{mem}) of C_6-NBD-PC associated with the SUV membranes (see Figure 7) are similarly plotted. Symbols are as defined in Figure 4. The fact that DMPC SUVs did not fuse even in 35 wt % PEG is indicated by the arrows pointing toward higher PEG concentrations.

When TMA-DPH was added to preformed SUVs, the fluorescence intensity increased rapidly to a plateau value within 30 min. Measurements were invariant for up to 24 h, even at probe/lipid ratios sufficiently high to cause self-quenching. This indicated that the probe, which has a charged polar head, remained associated with the vesicle outer leaflet during this time. Phase shift and modulation ratio data for SUVs prepared from different unsaturated PC species were all well described by a model assuming two lifetime components, as summarized in Table 1. The short component was roughly invariant between membranes, while the long component decreased with increasing chain unsaturation. In Figure 7B are plotted the long-lifetime components from these two-component descriptions as a function of the number of double bonds per lipid molecule. It is evident that PC species with double bonds only in the *sn*-2 fatty acid produced bilayers in which TMA-DPH showed a somewhat larger excited-state decay time (circles) than did PC species with double bonds in both fatty acid chains (squares). Comparison with the results presented in Figure 4 suggests an inverse correlation between TMA-DPH excited-state decay time and "fusogenicity". This inverse correlation is clearly revealed in Figure 8B. In this, we have plotted the TMA-DPH long fluorescence lifetime component as a function of the range of PEG concentrations for which fusion was first observed. TMA-DPH had the largest lifetime in DMPC SUV, which do not fuse at PEG concentrations up to 35 wt %. TMA-DPH lifetime decreased in SUV in proportion to the ease with which fusion could be induced, as evidenced by the decreasing PEG concentration needed to mediate fusion.

A decrease in TMA-DPH lifetime could imply either increased thermal motion of the probe and/or its environment or increased polarity of its environment. In order to distinguish between these two possibilities, we analyzed differential polarized phase shifts and modulation ratios in terms of a model for TMA-DPH motion involving free rotation in a restricted cone. We have shown that, if the dual lifetime nature of TMA-DPH fluorescence decay is taken into account, this model describes well the phase and modulation data (Lentz *et al.*, 1996). The parameters that describe this motion are as follows: ϕ, the rotational correlation time, which is the exponential decay constant describing the decay of fluorescence anisotropy to its asymptotic value, r_∞, after a pulsed excitation. The value of r_∞ approaches 0.4 for very small apical cone angles and approaches zero for un-inhibited rotation. Basically, it provides an order parameter for the orientation of TMA-DPH relative to the normal to the bilayer (Jähnig, 1979). The rate of probe diffusion is inversely related to both ϕ and r_∞. The parameters that describe TMA-DPH motion in terms of this model are presented in Table 1 for the several unsaturated lipids we have examined. The average value of ϕ was 1.3 $\pm$ 0.3, and there was no correlation evident between ϕ and the number of double bonds in a PC species or the concentration of PEG needed to promote fusion. The values of r_∞ for mixed-chain, unsaturated PC SUVs also showed no correlation with the degree of unsaturation (Figure 7C, open circles), but there was a marked difference in r_∞ for DOPC versus DLPC SUVs (Figure 7C, open squares). It was the difference between these two points that accounts for most of the correlation seen between r_∞ and the PEG concentration needed to promote fusion (Figure 8C). We conclude that, for doubly unsaturated (but not mixed-chain) PC species, increased chain unsaturation leads to an increased rate and extent of thermal motions in the upper regions of the bilayer.

It appears that the enhanced rate and extent of lipid motions in the bilayer interface region accounts for at least

Table 1: Summary of TMA-DPH Lifetime and Dynamics in Different Vesicles[a]

LIPID	τ_1 (ns)	f_1	τ_2 (ns)	τ_{AV} D_2O/H_2O	χ^2	ϕ	r_∞	χ^2
DLPC SUV	2.40 ± 0.014	0.813 ± 0.003	0.635 ± 0.014	1.11	1.9	1.41 ± 0.016	0.064 ± 0.004	0.3
DOPC SUV	3.39 ± 0.017	0.744 ± 0.002	0.719 ± 0.007	1.09	0.93	1.33 ± 0.030	0.106 ± 0.007	1.2
PAPC SUV	3.40 ± 0.042	0.852 ± 0.004	0.737 ± 0.023	1.09	2.5	0.97 ± 0.025	0.113 ± 0.007	1.9
PLPC SUV	3.80 ± 0.025	0.837 ± 0.002	0.793 ± 0.013	1.10	1.8	1.81 ± 0.034	0.114 ± 0.005	0.8
POPC SUV	4.09 ± 0.035	0.857 ± 0.003	0.791 ± 0.017	1.11	2.3	1.04 ± 0.042	0.118 ± 0.009	3.7
POPC LUV	4.44 ± 0.030	0.792 ± 0.002	1.11 ± 0.015	1.20	1.5	1.62 ± 0.035	0.090 ± 0.007	1.5
DMPC SUV	5.16 ± 0.076	0.819 ± 0.004	1.26 ± 0.027	1.29	6.7	1.55 ± 0.048	0.113 ± 0.008	2.8

[a] Component lifetimes were obtained by global analysis of two−four data sets for each sample, using the Globals Unlimited software. Goodness of fit is indicated by the reduced mean squared deviations of calculated from experimental values (χ^2); values close to 1 indicate an adequate description of the data. Parameter uncertainties are standard deviations.

some of the decrease in TMA-DPH fluorescence lifetime associated with the increased tendency of highly unsaturated PC SUVs to fuse. As noted above, however, the correlation between the extent of TMA-DPH motion and fusogenicity is non-existent for mixed-chain unsaturated PCs, although the strong correlation between fusogenicity and fluorescence lifetime persists for all unsaturated species (Figure 8B). Since the other environmental parameter that can lower lifetime is polarity, this implies that the environment of TMA-DPH becomes increasingly more polar in membranes with increasing tendencies to fuse. Ho *et al.* (1995) and Stubbs *et al.* (1995) have suggested the use of deuterium isotope exchange to detect exposure to water of a membrane probe having an exchangeable hydrogen, such as TMA-DPH. Stubbs *et al.* (1995) reported a 4.4% variation in the ratio of the fluorescence lifetime of TMA-DPH incorporated into LUVs in a D_2O buffer to that obtained in a H_2O buffer over the same range of unsaturation as examined here for SUVs. This ratio was measured to be 1.1 ± 0.01 for each of the membranes studied (Table 1). Thus, this measurement can not detect a difference in water exposure between SUVs having different extents of unsaturation. We noted elsewhere, however, that the D_2O/H_2O ratio for TMA-DPH seems to reflect more the penetration of probe into the membrane than the penetration of water (Lee & Lentz, 1996). This is evident in the fact that the ratio is greater in POPC LUV than in POPC SUV, for which water penetration must almost certainly be greater given the positive curvature stress experienced by SUV bilayer outer leaflets. We have recorded a similar result for DPPC LUVs versus SUVs (ratio = 1.11 versus 1.14). We conclude that TMA-DPH penetrates more deeply into SUV than into LUV bilayers. We conclude also that the similar D_2O/H_2O ratios observed for SUVs with different degrees of unsaturation indicate that the probe penetrates to similar depths into all these membranes, but that slight variations in depth of penetration could easily obscure variations in water penetration. It appears that the TMA-DPH D_2O/H_2O lifetime ratio is not capable of reporting the small increases in the extent of water penetration implied by the decrease in TMA-DPH lifetime that accompanies increased unsaturation of SUV component lipids.

DISCUSSION

The following conclusions result from this work:

(1) The Tb/DPA and the ANTS/DPX assays give identical fusion profiles for egg PC SUVs treated with increasing concentrations of PEG, thereby confirming the validity of both assays as used to follow PEG-mediated fusion.

(2) The observed fusion of egg PC and other unsaturated SUVs followed by the Tb/DPA assay demonstrates that fusion occurs in the dehydrated state in the presence of PEG.

(3) Increasing levels of acyl chain unsaturation in PCs used to prepare SUVs encourages both rupture and fusion, but fusion more than rupture. A clear correlation between SUV curvature and chain unsaturation appears to contribute to increased SUV fusogenicity.

(4) The effects of increasing chain unsaturation on SUV outer leaflet structure were different for mixed-chain versus doubly unsaturated PCs. The structural effect common to inducing fusion in both types of unsaturated PC SUVs is probably increased penetration of the upper region of the bilayer by water molecules, leading to a thermodynamically unstable interface. The first three conclusions are self-evident; the fourth is discussed below.

We have previously noted that the PEG concentration at which fusion is first observed reflects the inter-bilayer distance at which juxtaposed bilayers can form a fusion intermediate (Burgess *et al.*, 1992). Based on fusion measurements with phosphatidylcholine/phosphatidylethanolamine mixed vesicles, we suggested that fusion might occur at the point of molecular contact (roughly a 5-Å inter-bilayer water layer at 35 wt % PEG for DOPC vesicles) or at a larger inter-bilayer separation if approaching bilayer leaflets were sufficiently thermodynamically destabilized (Burgess *et al.*, 1992). The parameters characterizing membrane−membrane hydration repulsion vary little with acyl chain unsaturation within the same lipid class (Rand & Parsegian, 1989). These observations argue that unsaturated PC SUVs were probably not in molecular contact at the low PEG concentrations needed to fuse these vesicles (Figure 4). It would appear, then, that the substantial increase in fusogenicity that accompanies chain unsaturation reflects increased destabilization of approaching leaflets.

Our results suggest that outer leaflet destabilization of SUVs prepared from unsaturated PCs probably results from three structural effects, depending on the nature of the PC species constituting the SUV bilayer. The first is increased membrane curvature (Figure 8A). The asymmetric packing strain associated with extreme curvature is well documented (Sheetz & Chan, 1972; Suurkuusk *et al.*, 1976; Huang & Mason, 1978; Bramhall, 1986; Teissié, 1987; Schuh *et al.*, 1982). Probably as a result, SUVs fuse readily below the order/disorder lamellar phase transition (Suurkuusk *et al.*, 1976; Lichtenberg *et al.*, 1981) and even slowly in the fluid phase (Lentz *et al.*, 1987). The increased membrane curvature of SUV bilayers certainly increases outer-leaflet free volume, as illustrated by the fact that the fraction of C_6-NBD-PC partitioning (at a lipid/probe = 500) into disaturated PC SUVs was increased to 0.59 (Figure 6) from 0.47 in disaturated PC LUVs (Lee & Lentz, 1997). However, dipalmitoylphosphatidylcholine SUVs are also highly

curved (1/radius = 0.059, comparable to DLPC SUVs-Figure 7A), and disaturated PC SUVs still do not fuse at PEG concentrations below which rupture occurs (Lentz *et al.*, 1992). Thus, chain unsaturation appears to be crucial to SUV fusion in ways other than increasing curvature.

The second structural effect appears to be increased free volume and thermal motion in the upper regions of the contacting outer leaflets of fusogenic bilayers. We report elsewhere that fusogenic perturbations of LUV outer leaflets due to lipid shape change or lipid removal also lead to increased TMA-DPH motion (Lee & Lentz, 1997). In this latter case, the destabilizing manipulations also created free volume into which C_6-NBD-PC partitioned more readily than into non-fusogenic, unperturbed bilayers. Apparently, increased unsaturation of both chains also increases thermal motion (squares in Figure 7C) and increases free volume (squares in Figure 7D) in the upper regions of doubly unsaturated PC SUVs. The increase in fusogenicity with increased unsaturation in doubly unsaturated PC SUVs probably reflects this dependence of fusogenicity on molecular order and packing within the upper regions of contacting outer leaflets.

In the case of mixed-chain PCs, increased unsaturation actually decreased partitioning of C_6-NBD-PC into the bilayer (Figure 7D) and had no effect on the thermal motion of TMA-DPH (Figure 7C). Similarly, increased unsaturation in the *sn*-2 position of mixed-chain PCs reduced the ^{2}H-NMR order parameter mainly in the upper regions of the bilayer, without altering order in the center of the bilayer (Separovic *et al.*, 1996). These observations suggest that a single unsaturated fatty acid in the *sn*-2 position somehow restricts chain packing. Consistent with this, C_6-NBD-PC also partitions less readily into unsaturated as compared to saturated PC SUVs (Figure 6). Nonetheless, SUVs prepared from mixed-chain PCs still fused, and increased chain unsaturation still led to increased fusogenicity. A third structural effect is thus needed to explain the increase of fusogenicity with increased unsaturation in mixed-chain PCs. We propose that this effect is increased partitioning of water into the interface region of the bilayer. Since TMA-DPH seems to partition to roughly the same depth into all the SUV membranes we have compared (constant D_2O/H_2O ratio, see Results and Table 1), the strong correlation between TMA-DPH lifetime and unsaturation (Figure 7B) suggests that the polarity of the bilayer upper region increases with increasing unsaturation, consistent with increased water penetration. Stubbs *et al.* (1995) have also suggested that such deceases in lifetime might be a measure of increased water penetration into unsaturated bilayers. Apparently, increased unsaturation of the *sn*-2 chain in mixed-chain PCs creates packing defects that allow penetration of a small molecule such as water, but not a large molecule such as C_6-NBD-PC, into the upper regions of the bilayer. Thus, our results with mixed-chain PC SUVs suggest that water penetration into the upper regions of contacting bilayer outer leaflets is crucial to membrane fusion.

What, then, is the role of membrane curvature and decreased packing density in the interface region in producing the bilayer destabilization that leads to fusion? We suggest that increased membrane curvature and decreased lipid packing both favor increased water penetration and that the increased contact between water and hydrocarbon results in a higher surface free energy (surface tension). Thus, we suggest that the key event leading to fusion is the thermodynamic destabilization of contacting outer leaflets resulting from increased water penetration. This might favor formation of some structure that deviates from the lamellar motif and that serves as a fusion intermediate. At present, we favor the "stalk" intermediate proposed by Chernomordik and colleagues (1995).

REFERENCES

Arnold, K., Zschoernig, O., Bacthel, D., & Herold, W. (1990) *Biochim. Biophys. Acta 1022*, 303−310.

Bailey, F. E., & Koleske, J. V. (1967) in *Nonionic Surfactants* (Schick, M. J., Ed.) pp 794−822, Marcel Dekker, New York.

Bramhall, J. (1986) *Biochemistry 25*, 3479−3486.

Burgess, S. W., Massenburg, D., Yates, J., & Lentz, B. R. (1991) *Biochemistry 30*, 4193−4200.

Burgess, S. W., McIntosh, T. J., & Lentz, B. L. (1992) *Biochemistry 31*, 2653−2661.

Chernomordik, L., Chanturiya, A., Green, J., & Zimmerberg, J. (1995) *Biophys. J. 69*, 922−929.

Ellens, H., Bentz, J., & Szoka, F. C. (1984) *Biochemistry 23*, 1532−1538.

Evans, E., & Needham, D. (1988) *Macromolecules 21*, 1822−1831; cf. a similar article in *Molecular mechanisms of membrane fusion* (Ohki, S., Ed.) pp 83−100, Plenum, New York.

Ho, C., Slater, S. J., & Stubbs, C. D. (1995) *Biochemistry 34*, 6188−6195.

Horrocks, W. DeW., Jr., & Sudnick, D. R. (1979) *J. Am. Chem. Soc. 101*, 334−340.

Huang, C., & Mason, J. T. (1978) *Proc. Natl. Acad. Sci. U.S.A. 75*, 308−310.

Jähnig, F. (1979) *Proc. Natl. Acad. Sci. U.S.A. 76*, 6361−6365.

Lee, J.-K., & Lentz, B. R. (1997) *Biochemistry 36*, 421−431.

Lentz, B. R. (1994) *Chem. Phys. Lipids 73*, 91−106.

Lentz, B. R., Carpenter, T. J., & Alford, D. R. (1987) *Biochemistry 26*, 5389−5397.

Lentz, B. R., McIntyre, G. F., Parks, D. J., Yates, J. C. (1992) *Biochemistry 31*, 2643−2653.

Lentz, B. R., Wu, J. R., Zheng, L.-X., & Převrátil, J. (1996) *Biophys. J. 71*, 3302−3313.

Lentz, B. R., Talbot, W., Lee, J.-K., & Zheng, L. X. (1997) *Biochemistry 36*, 2076−2083.

Lichtenberg, D., Friere, E., Schmidt, C. F., Barenholtz, Y., Felgner, P. L., & Thompson, T. E. (1981) *Biochemistry 20*, 3462−3467.

Massenburg, D., & Lentz, B. R. (1993) *Biochemistry 32*, 9172−9180.

Mayer, L. D., Hope, M. J., & Cullis, P. R. (1986) *Biochim. Biophys. Acta 858*, 161−168.

Parente, R. A., & Lentz, B. R. (1986) *Biochemistry 25*, 6678−6688.

Rand, R. P., & Parsegian, V. A. (1989) *Biochim. Biophys. Acta 988*, 351−376.

Schullery, S. E., Schmidt, C. F., Felgner, P., Tillack, T. W., & Thompson, T. E. (1980) *Biochemistry 19*, 3919−3923.

Separovic, F., & Gawrisch, K. (1996) *Biophys. J. 71*, 274−282.

Sheetz, M. P., & Chan, S. I. (1972) *Biochemistry 11*, 4573−4581.

Shuh, J. R., Banerjee, U., Müller, L., & Chan, S. I. (1982) *Biochim. Biophys. Acta 687*, 219−225.

Stubbs, C. D., Ho, C., & Slater, S. J. (1995) *J. Fluorescence 5*, 19−28.

Suurkuusk, J., Lentz, B. R., Barenholz, Y., Biltonen, R. L., & Thompson, T. E. (1976) *Biochemistry 15*, 1393−1401.

Teissié, J. (1987) *Biochemistry 26*, 840−846.

Viguera, A. R., Mencia, M., & Goni, F. M. (1993) *Biochemistry 32*, 3708−3713.

Wilschut, J., Duzgunes, N., & Papahadjopoulos, D. (1980) *Biochemistry 19*, 6011−6021.

Wu, H., Zheng, L-X., & Lentz, B. R. (1996) *Biochemistry 35*, 12602−12611.

Wu, J. R., & Lentz, B. R. (1994) *J. Fluorescence 4*, 153−163.

BI962437I